A Novel Junction Temperature Estimation Method Independent of Bond Wire Degradation for IGBT

Yanyong Yang, *Member, IEEE*, Xiaofeng Ding, *Member, IEEE*, and Pinjia Zhang, *Senior Member, IEEE*

***Abstract*—The insulated-gate bipolar transistor (IGBT) junction temperature is crucial for condition monitoring, reliability assessment, and health management. However, the existing IGBT temperature monitoring methods are affected by the aging of IGBT bond wires. A novel junction temperature estimation method independent of bond wire degradation for IGBT is proposed in this article. On-state voltage drop and turn-ON gate voltage overshoot are analyzed for dependence on the junction temperature and bond wire degradation. These two temperature and bond wire monitoring electrical parameters are combined by the artificial neural network, to eliminate the effect of bond wire degradation. A double pulse test platform is built to verify the influence of temperature and bond wire degradation on on-state voltage drop and turn-ON gate voltage overshoot, which agrees with the theoretical analysis. Lots of experimental data at various collector-emitter voltages, load currents, IGBT junction temperature, and bond wire degradation are tested. A BP neural network is trained for junction temperature monitoring and its optimal number of hidden layers is studied. The experimental results show that the junction temperature estimation method based on the neural network can effectively eliminate the effect of bond wire degradation. The estimation error is around 4.219 °C. The proposed method has the advantages of high accuracy and a wide application range for junction temperature monitoring.**

***Index Terms*—Artificial neural network (ANN), insulated-gate bipolar transistor (IGBT), monitoring, power semiconductor devices, reliability, temperature measurement.**

NOMENCLATURE

α_{PNP}	Gain of the inherent bipolar transistor.
C_{I}	Unit-area isolation capacitance.
C_{OX}	Specific capacitance of the gate oxide.
d	Half-drift region thickness.
D_{a}	Ambipolar diffusion coefficient.
d_{b}	Diameter of the bond wire (in nanometers).
e_0	Elementary charge.
ε_{s}	Permittivity of the semiconductor.
G_{m}	Transconductance.
i_{g}	Gate driver current.
i_{c}	Collector current.
I_{L}	Stable load current.
J_{C}	Collector current density.
k	Boltzmann's constant.
L_{s}	Parasitic self-inductance of one bond wire.
L_{CH}	Channel length.
L_{a}	Ambipolar diffusion length.
l	Length of the bond wire (in millimeters).
L_{i}	Parasitic inductance of bond wire i.
$L_{\text{s_i}}$	Self-inductance of bond wire i.
L_{e}	Parasitic inductance.
M	Parasitic mutual inductance of one bond wire.
M_{ij}	Mutual inductances between bond wire i and j.
n	Number of effective bond wires.
n_{i}	Intrinsic carrier concentration.
N_{A}	Acceptor impurity concentration.
p	Cell pitch.
q	Charge of the electron.
R_{bond}	Parasitic resistance of a bond wire.
$R_{\text{g_out}}$	Externally connected gate resistor.
s	Distance between two bond wire centers (in millimeters).
T	IGBT junction temperature.
τ_{HL}	High-level lifetime in the drift region.
μ_{n}	Electron mobility for silicon.
μ_{ni}	Inversion layer mobility.
μ_{p}	Hole mobility for silicon.
$V_{\text{g_p}}$	Gate voltage overshoot.
V_{FB}	Flatband voltage.
v_{g}	Gate driver voltage.
v_{ce}	Collector-emitter voltage of IGBT.
V_{bus}	Dc bus voltage.
$V_{\text{g_th}}$	Gate threshold voltage.
V_{IGBT}	On-state voltage drop between the power collector terminal and emitter of IGBT.
$V_{\text{IGBT_chip}}$	On-state voltage drop of the IGBT chip.
$V_{\text{IGBT_bond}}$	Voltage drop of bond wires.
W_{N}	Width of the N-base region.
$\frac{W}{L}$	Ratio between the width and the length of the MOS channel.
ψ_{B}	Fermi level from the intrinsic Fermi level.

Manuscript received 24 October 2022; revised 4 February 2023 and 19 March 2023; accepted 3 May 2023. Date of publication 8 May 2023; date of current version 21 June 2023. This work was supported in part by the National Key R&D Program of China under Grant 2022YFB2405300, in part by the National Natural Science Foundation of China under Grants 52207185, 52225702, and 51877006, in part by the China Postdoctoral Science Foundation under Grant 2022M720343, and in part by Project (SKLD22KZ03) supported by State Key Laboratory of Power System and Generation Equipment. Recommended for publication by Associate Editor K. Wada. *(Corresponding authors: Xiaofeng Ding; Pinjia Zhang.)*

Yanyong Yang and Xiaofeng Ding are with the Department of Electrical Engineering, Beihang University, Beijing 100191, China (e-mail: yyy18@mails.tsinghua.edu.cn; dingxiaofeng@buaa.edu.cn).

Pinjia Zhang is with the Department of Electrical Engineering, Tsinghua University, Beijing 100084, China (e-mail: pinjia.zhang@ieee.org).

Color versions of one or more figures in this article are available at https://doi.org/10.1109/TPEL.2023.3274126.

Digital Object Identifier 10.1109/TPEL.2023.3274126

I. Introduction

POWER electronics technology is widely used in all aspects of industrial life, such as electric vehicles, new energy generation, dc transmission converter valves, etc [1]. Power electronic power device is the core component of power electronic converter, and its failure rate accounts for 31% [2], which is the highest among all components. The main stress of the device is thermal stress, accounting for 55% [3]. The insulated-gate bipolar transistor (IGBT) is one of the most widely used power electronic devices, so it is of great significance to monitor the junction temperature of IGBT online.

There are many temperature monitoring methods, such as thermal impedance network-based, infrared imaging-based, temperature sensor-based measurement, and temperature-sensitive electrical parameters-based methods. Among these methods, the methods based on temperature-sensitive electrical parameters are the most attractive [4]. The existing IGBT junction temperature monitoring methods based on temperature-sensitive electrical parameters can be roughly divided into four categories according to their signal types. Namely, voltage signals-based methods, current signals-based methods, other signals-based methods, and electrical parameters combined with artificial intelligence methods.

For the monitoring circuit, measuring voltage is direct and convenient. There have been a lot of researches on voltage signals-based methods. The traditional one is on-state voltage drops under a large current-based method [5], [6], [7]. However, it is influenced by bond wire degradation. Besides, the on-state voltage drop under a small current is utilized for IGBT junction temperature and it is less affected by the bond wire failure [6]. However, the small currents often need to be injected extra, which is intrusive. In terms of gate voltage, gate threshold voltage [8], gate flatband voltage [9], gate prethreshold voltage [10], and gate miller plateau voltage [11], [12] are proposed for IGBT junction temperature monitoring. However, because of the small voltage range of gate voltage, they have a low resolution for temperature monitoring. Turn-OFF collector voltage rate dv_{ce}/dt is measured for IGBT junction temperature estimation [13], [14]. However, it is difficult to measure dv_{ce}/dt accurately online in practice. The voltage between the power emitter and kelvin emitter terminals is proposed in [15] for IGBT junction temperature monitoring. Nevertheless, its resolution is relatively low.

Many current signals-based methods have been proposed to monitor IGBT junction temperature. Collector saturation current under constant gate voltage is studied for IGBT junction temperature estimation [8], [16], [17]. However, changing the gate voltage or implementing a short saturation current test can have an intrusive effect on device operation in practice. More importantly, the saturation current is closely related to the condition of IGBT bond wires. The dependence of leakage current on IGBT junction temperature is studied in [18] and [19]. However, it is difficult to accurately measure the leakage current of IGBT during the blocking state in practice. In terms of gate current, peak gate current [20], [21] and internal gate resistance via peak gate current [22] are utilized for IGBT junction temperature estimation. However, they might be affected by bond wire degradation and are difficult to be measured. Moreover, turn-ON di_{c}/dt [23], [24], [25], turn-OFF collector current di_{c}/dt [15], and collector tail current [11] are proposed for IGBT junction estimation. However, the measurement of these temperature-sensitive parameters requires a high-frequency sampling circuit and a very high-speed operation circuit, which increases the system's cost.

In addition to monitoring methods based on voltage and current signals, there are IGBT junction temperature technologies based on other signals. Transconductance is studied for IGBT junction temperature monitoring [11]. However, estimation of transconductance requires measurement of collector current as well as gate voltage, which increases measurement complexity. Besides, transconductance is influenced by bond wire degradation. Gate miller plateau width is proposed in [13] for junction temperature monitoring. However, the gate miller plateau width is strongly related to the bond wire degradation and it is used for bond wire detection [26]. Turn-ON delay time [23] and turn-OFF time [27] are utilized for IGBT junction temperature monitoring. However, there are limitations in practical implementation for measuring a short switching delay time. In practice, due to the additional transmitter circuit of current and time-related signals, current and other signals-based methods require higher effort to calculate the temperature in comparison to the voltage signals-based method voltage.

Electrical parameters combined with artificial intelligence methods can fully utilize the dependence between electrical parameters and IGBT junction temperature. A large amount of data is used for preliminary training, to achieve high-precision IGBT temperature monitoring. A reference model has been developed with combining four temperature-sensitive electrical parameters [28]. However, measuring four parameters at the same time increases the complexity of the monitoring system in practical application. Support vector regression, random forest, and backpropagation neural network are constructed to estimate the junction temperature of IGBT [29]. The error backpropagation (BP) neural network model was established by using the on-state voltage drop to predict the junction temperature [30]. An online IGBT junction temperature extraction system based on BP neural network related to the saturation collector-emitter voltage and turn-OFF delay time is presented in [31]. However, the work in [29], [30], and [31] do not consider the influence of IGBT bond wire degradation.

As can be seen from the above-mentioned introduction, a fundamental shortcoming is that many seemingly feasible methods are affected by IGBT bond wire degradation. The aging of IGBTs is inevitable as the service progresses. The degradation of bond wires is the most common failure in IGBT modules [32]. Therefore, how to avoid the influence of bond wire degradation to be suitable for long-term IGBT junction temperature monitoring is a very tricky problem. However, the temperature monitoring of IGBT with decoupling bond wire failure cannot be achieved by relying on a single temperature-sensitive parameter.

To address the above-mentioned problems, a novel junction temperature estimation method independent of bond wire

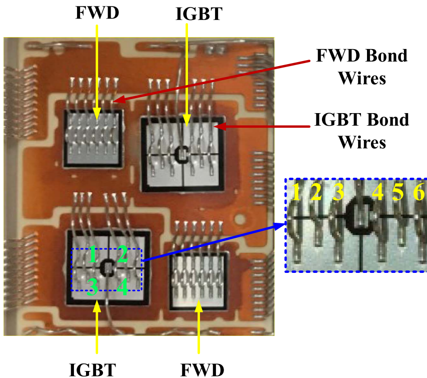

Fig. 1. Appearance of the IGBT module after removing the top shell.

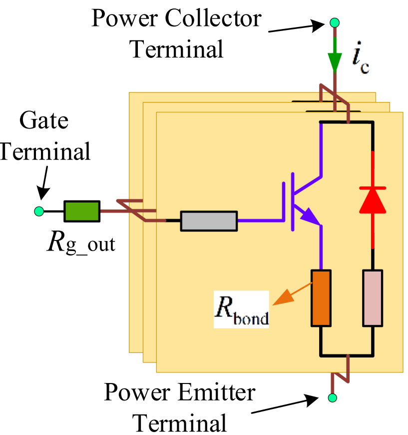

Fig. 2. Circuit considering parasitic resistance of bond wires of 3 parallel chips.

degradation for IGBT is proposed in this article. The on-state voltage drop and turn-ON gate voltage overshoot are affected by both the IGBT junction temperature and bond wire degradation. There are nonlinear relationships between on-state voltage drop and bond wire degradation, as well as between turn-ON gate voltage overshoot and bond wire degradation. It is difficult to establish a mathematical analytical model to combine the two electrical parameters to decouple the bond wire degradation. In this article, these two electrical parameters are combined by a neural network, which can eliminate the influence of bond wire and accurately monitor the junction temperature of IGBT. The method proposed has the advantages of being noninvasive, high precision, and independent of bond wire degradation.

The rest of this article is organized as follows. In Section II, the dependencies of IGBT on-state voltage drop and turn-ON gate voltage overshoot on junction temperature and bond wire degradation are analyzed. The neural network used in this article is presented. In Section III, the experiment setup and results are presented. The influence of junction temperature and bond wire degradation on IGBT on-state voltage drop and turn-ON gate voltage overshoot is verified. The prior experimental data at various operation conditions are measured for training the neural network. The measuring circuit is introduced. Moreover, the practical implementation and verification with the neural network are illustrated. Finally, Section IV summarizes the conclusion.

II. Junction Temperature Estimation Method Independent of Bond Wire Degradation

A. *On-State Voltage Drop Affected by Temperature and Bond Wire Failure*

For the device under test (DUT) in this article, the appearance of the IGBT module after removing the top shell is shown in Fig. 1.

The IGBT bond wires are usually aluminum and they connect the IGBT chips to the copper bar. Besides, Fig. 1 illustrates that each IGBT chip includes 4 zones. In total, 6 bond wires are divided into 2 groups, which are separately connected with zone 1, 3, and zone 2, 4. Furthermore, considering three bond wires lift-off for example. If the three bond wires lift-off are 1, 2, and 3, zone 1, and 3 will be offline. However, if the three bond wires lift-off are 1, 2, and 6, four zones of IGBT will still be online. If there are IGBT zones out of operation, the equivalent current density of the effective IGBT zone will be twice as much as it should be. Thus, the on-state voltage drop of IGBT will significantly increase compared to that under all zones being effective.

Besides, each IGBT of DUT is composed of 3 parallel IGBT chips, which are symmetrical. During the steady state of IGBT on-state, the parasitic resistance of bond wires will affect the on-state voltage drop. Hence, the circuit considering the parasitic resistance of bond wires of 3 parallel chips is shown in Fig. 2.

The parasitic resistances of bond wires are closely related to the status of bond wires. Besides, the position where the bond wire lifts off also affects the on-state characteristics of IGBT.

The on-state voltage drop V_{IGBT} between power collector terminal and emitter of IGBT can be expressed as follows:

$$V_{\mathrm{IGBT}} = V_{\mathrm{IGBT_chip}} + V_{\mathrm{IGBT_bond}}. \tag{1}$$

The on-state voltage drop of the IGBT chip is determined by [33]

$$V_{\mathrm{IGBT_chip}} = \frac{2kT}{q}\left(\ln\left(J_{\mathrm{C}}W_{\mathrm{N}}\right) - \ln\left(4qD_{\mathrm{a}}n_{\mathrm{i}}\frac{\left(\frac{W_{\mathrm{N}}}{2L_{\mathrm{a}}}\right)\tanh\left(\frac{W_{\mathrm{N}}}{2L_{\mathrm{a}}}\right)}{\sqrt{1-0.25\tanh^4\left(\frac{W_{\mathrm{N}}}{2L_{\mathrm{a}}}\right)}}\right)\right) + \frac{4d^2}{\left(\mu_{\mathrm{n}}+\mu_{\mathrm{p}}\right)\tau_{\mathrm{HL}}} + \frac{pL_{\mathrm{CH}}J_{\mathrm{C}}}{\mu_{\mathrm{ni}}C_{\mathrm{OX}}\left(V_{\mathrm{ge}}-V_{\mathrm{g_th}}\right)}. \tag{2}$$

On the other hand, the on-state voltage drop of bond wires can be expressed as follows:

$$V_{\mathrm{IGBT_bond}} = i_{\mathrm{c}}R_{\mathrm{bond}}. \tag{3}$$

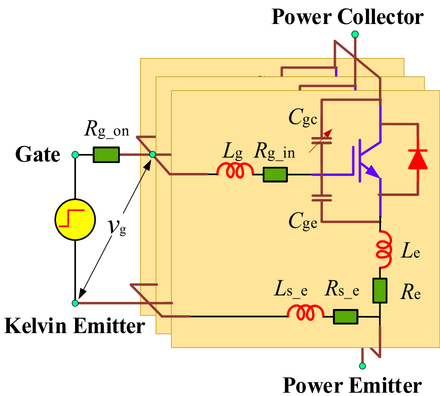

Fig. 3. Equivalent gate driver loop circuit of IGBT [34].

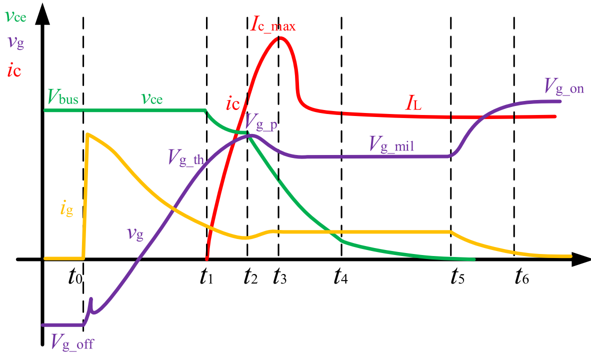

Fig. 4. Waveforms of IGBT turn-ON transient.

Replacing the variables in (1) with (2) and (3), the on-state voltage drop V_{IGBT} can be given by

$$V_{\mathrm{IGBT}} = \frac{2kT}{q}\left(\ln\left(J_{\mathrm{C}}W_{\mathrm{N}}\right) - \ln\left(4qD_{\mathrm{a}}n_{\mathrm{i}}\frac{\left(\frac{W_{\mathrm{N}}}{2L_{\mathrm{a}}}\right)\tanh\left(\frac{W_{\mathrm{N}}}{2L_{\mathrm{a}}}\right)}{\sqrt{1-0.25\tanh^{4}\left(\frac{W_{\mathrm{N}}}{2L_{\mathrm{a}}}\right)}}\right)\right) + \frac{4d^2}{\left(\mu_{\mathrm{n}}+\mu_{\mathrm{p}}\right)\tau_{\mathrm{HL}}} + \frac{pL_{\mathrm{CH}}J_{\mathrm{C}}}{\mu_{\mathrm{ni}}C_{\mathrm{OX}}\left(V_{\mathrm{ge}}-V_{\mathrm{g_th}}\right)} + i_{\mathrm{c}}R_{\mathrm{bond}}. \tag{4}$$

Therefore, V_{IGBT} is dependent on the junction temperature of the IGBT and the status of the IGBT bond wire, while the temperature variable and bond wire state variable are independent of each other. In other words, the temperature of the IGBT module does not affect the state of the bond wires, and the lift-off of the bond wires will not affect the temperature. IGBT temperature monitoring only based on the on-state voltage drop will make the error increase with the failure of the IGBT bond wire. It is difficult to use a simple mathematical formula to characterize the relationship between the on-state voltage drop of IGBT and the degree of bond wire failure. Besides, the relationship between the number of bond wire lift-off and on-state voltage drop V_{IGBT} is nonlinear.

B. Turn-On Gate Voltage Overshoot Affected by Temperature and Bond Wire Failure

Considering the IGBT module FF300R12ME4 in this article, the equivalent gate driver loop circuit is shown in Fig. 3 [34].

During the switching duration, the stray inductance of emitter bond wires will influence the dynamic process in the gate charge loop circuit. The main waveforms of IGBT during a turn-ON transient are shown in Fig. 4.

In Fig. 4, I_{L} flows through the collector of IGBT after the turn-ON process. When the gate voltage increases to $V_{\mathrm{g_th}}$ at t_1, the IGBT collector current i_{c} begins to increase. In the period of $(t_1 - t_2)$, i_{c} increases to I_{L} with a high current change rate $\frac{di_{\mathrm{c}}}{dt}$.

According to [35], the partial inductance of bond wire consists of partial self-inductance and mutual inductance. L_{s} can be determined by the following equation:

$$L_{\mathrm{s}} = 2\cdot 10^{-1}\cdot l\cdot\left[\ln\left(4\cdot 10^{3}\cdot\frac{l}{d_{\mathrm{b}}}\right) - 0.75\right] \tag{5}$$

where M can be determined by

$$M = 0.19685\cdot d_{\mathrm{b}}\left[\ln\left(\frac{2l}{s}\right) - 1 + \frac{s}{l} - \left(\frac{s}{2l}\right)^{2}\right]. \tag{6}$$

For multiple bond wires, the mutual inductance is caused by the magnetic coupling of multiple bond wires. Therefore, the parasitic inductance L_{i} of bond wire i can be expressed as follows:

$$L_{\mathrm{i}} = L_{\mathrm{s_i}} + \sum_{j=1}^{j=n} M_{\mathrm{ij}}(j \neq i). \tag{7}$$

For a typical value, the total stray inductance of one chip is 2.55 nH at a healthy state and 4.57 nH at 2 bond wires remaining [34].

During the period of $(t_1 - t_3)$, the current change rate $\frac{di_{\mathrm{c}}}{dt}$ would be more than 1000 A/us [9], [25]. $V_{\mathrm{g_p}}$ is strongly influenced by the induced voltage across L_{e} of collect current change rate $\frac{di_{\mathrm{c}}}{dt}$. Theoretically speaking, $V_{\mathrm{g_p}}$ is also related to the voltage drop when i_{c} flows across the resistance R_{e} of emitter bond wires, the induced voltage across the parasitic inductance L_{e} of gate current change rate $\frac{di_{\mathrm{g}}}{dt}$, the voltage drop when i_{g} flows across the gate loop resistance of bond wires. However, those elements can be neglected because they are tiny compared with the induced voltage across the parasitic inductance L_{e} of collect current change rate $\frac{di_{\mathrm{c}}}{dt}$ [34]. Hence, the gate voltage overshoot $V_{\mathrm{g_p}}$ can be simplified into the following equation:

$$V_{\mathrm{g_p}} = V_{\mathrm{g_th}} + L_{\mathrm{e}}\frac{di_{\mathrm{c}}}{dt}. \tag{8}$$

According to [11], $V_{\text{g_th}}$ can be determined by the following equation:

$$V_{\text{g_th}} = V_{\text{FB}} + 2 \cdot \psi_{\text{B}}(T) + \frac{\sqrt{4\varepsilon_{\text{s}} e_0 N_{\text{A}} \psi_{\text{B}}(T)}}{C_{\text{I}}} \tag{9}$$

where ψ_{B} is determined by the following equation [11]:

$$\psi_{\text{B}}(T) = \frac{k \cdot T}{e_0} \cdot \ln\left(\frac{N_{\text{A}}}{n_i(T)}\right). \tag{10}$$

In (10), $n_{\text{i}}$is influenced by the IGBT junction temperature T. On the other hand, the turn-ON current change rate $\frac{di_{\text{c}}}{dt}$ can be determined as follows [23], [25]:

$$\frac{di_{\text{c}}}{dt} = \frac{dv_{\text{g}}}{dt} \cdot G_{\text{m}} = \frac{dv_{\text{g}}}{dt} \cdot \left[\frac{1}{1 - \alpha_{\text{PNP}}(T)}\right] \cdot \left[\mu_{\text{n}} \cdot C_{\text{ox}} \cdot \frac{W}{L} \cdot (v_{\text{g}} - V_{\text{g_th}})\right]. \tag{11}$$

According to [23], the turn-ON current change rate $\frac{di_{\text{c}}}{dt}$ rises with the increase of both bus voltage V_{bus} and load current I_{L}, and it decreases with the increase of IGBT junction temperature T.

Combining the above-mentioned equations, the gate voltage overshoot $V_{\text{g_p}}$ can be determined as follows:

$$V_{\text{g_p}} = V_{\text{FB}}(T, V_{\text{bus}}) + 2 \cdot \frac{k \cdot T}{e_0} \cdot \ln\left(\frac{N_{\text{A}}}{n_i(T)}\right) + \frac{\sqrt{4\varepsilon_{\text{s}} e_0 N_{\text{A}} \left(\frac{k \cdot T}{e_0} \cdot \ln\left(\frac{N_{\text{A}}}{n_i(T)}\right)\right)}}{C_{\text{I}}} + L_{\text{e}} \cdot \frac{dv_{\text{g}}}{dt} \cdot \left[\frac{1}{1 - \alpha_{\text{PNP}}(T)}\right] \cdot \left[\mu_{\text{n}} \cdot C_{\text{ox}} \cdot \frac{W}{L} \cdot (v_{\text{g}} - V_{\text{g_th}})\right]. \tag{12}$$

Equation (12) indicates that the gate voltage overshoot $V_{\text{g_p}}$ is affected by dc bus voltage V_{bus}, load current I_{L}, especially IGBT junction temperature T, and IGBT stray emitter inductance. In (12), the temperature variable and bond wire state variable are independent of each other.

Equation (12) shows that the relationships between the number of bond wire lift-off and gate voltage overshoot $V_{\text{g_p}}$ is nonlinear. Besides, the relationships between the junction temperature and gate voltage overshoot $V_{\text{g_p}}$ is nonlinear.

Since both relationships of (4) and (12) contain independent variables of temperature and bond wire state, one of the variables can be eliminated by combining two relationships. In this article, by combining the relationships (4) and (12), the influence of the bond wire state on temperature monitoring can be eliminated. However, because of the nonlinear relationships between the number of bond wire lift-off and the on-state voltage drop as well as the gate voltage overshoot $V_{\text{g_p}}$, there is no exact analytical function to describe the relationship between the on-state voltage and gate voltage overshoot and the degree of bond wire failure.

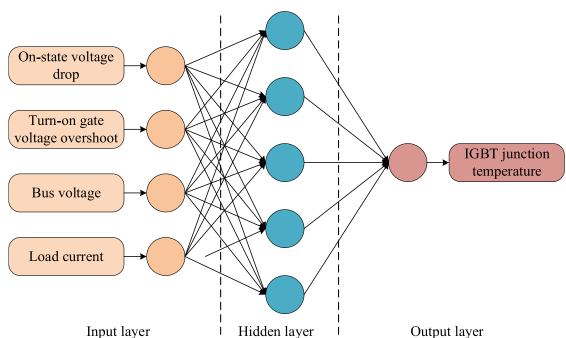

Fig. 5. BP neural network structure for IGBT temperature monitoring.

C. Neural Network for Junction Temperature Estimation Independent of Bond Wire Degradation

The artificial neural network (ANN) is an algorithmic mathematical model that simulates the behavior characteristics of an animal neural network for distributed and parallel information processing. ANN can realize the nonlinear mapping relationship by adjusting the internal and the relationship between a large number of nodes. The error BP multilayer feedforward neural network (BP neural network) is a kind of algorithm that can best embody the nature of an ANN [30]. BP neural network is based on gradient descent and has strong nonlinear mapping ability. Therefore, BP neural network is used to monitor IGBT temperature in this article for eliminating the effect of the bond wire. The BP neural network structure for IGBT temperature monitoring is shown in Fig. 5.

BP neural network has an input layer, hidden layer, and output layer. The on-state voltage drop, turn-ON gate voltage overshoot, collector-emitter voltage, and load current of IGBT are used as input signals of the input layer. The IGBT junction temperature is used as the output signal of the output layer. In network training, different hidden layers are changed to make the trained network show the best performance.

In the process of training the BP neural network model, the original experimental data is divided into three parts, namely the training set, test set, and validation set. The training set accounts for 70% of the total data, and it is a set of samples used for training, mainly used to train the parameters in the neural network. The test set accounts for 15% of the total data, and it is used to evaluate the performance of neural network objectively. And the validation set accounts for 15% of the total data, and it is used to verify and compare the performance of various models.

With the method proposed, there is no need to build complex mathematical models for solving the IGBT junction temperature. BP neural network turns the preliminary experimental data used for calibration into the self-learning network. Therefore, the method proposed has the advantages of fast calculation speed, high calculation accuracy, and self-adaptation for nonlinear mapping.

III. Experiment Setup and Verification

A. Experimental Setup

The double pulse test is the most commonly used verification experiment [9], [10], [11], [12], [20], [22], [24], [27], [28]. The

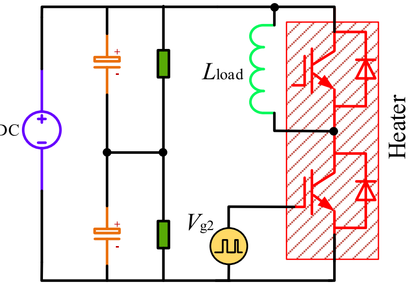

Fig. 6. Scheme of the double-pulse test.

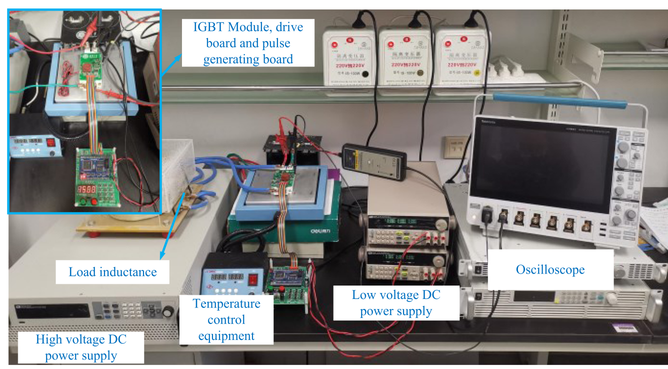

Fig. 7. Prototype of the double-pulse experiment platform.

TABLE I
INSTRUMENT AND TYPE OF THE DOUBLE-PULSE EXPERIMENT PLATFORM

Instrument	Type
Pulse generator	TMS320F28335
Mixed-signal oscilloscope	MSO46
Load	Air-core inductor of 1.5 mH
Bus capacitance	5000 uF, realized by two 10000 uF capacitors in series
Differential voltage probe	700924 of Yokogawa
Rogowski Coil probe	CP9060S
High voltage DC source	IT6012D-800-50
Auxiliary low-voltage power supply	IT6322A

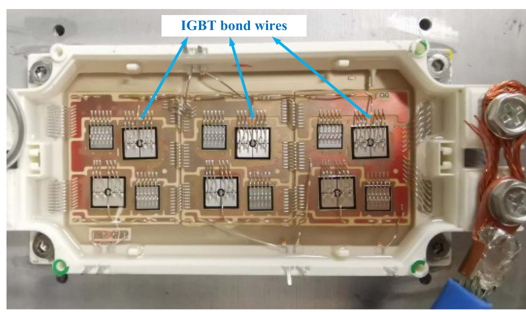

Fig. 8. IGBT module with the cover removed.

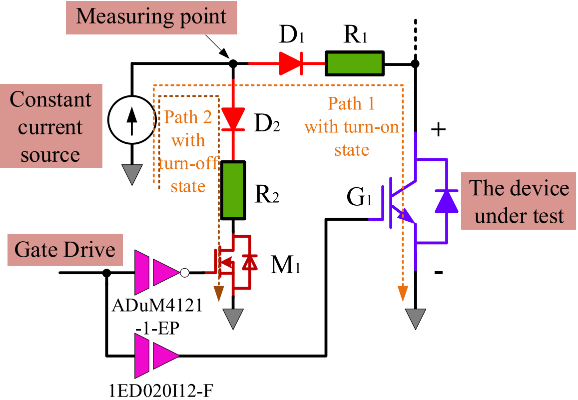

Fig. 9. Online monitoring circuit of IGBT on-state voltage drop.

voltage and current of the DUT can be set over a wide range. Therefore, a double-pulse test platform is built and experiments are conducted to verify the IGBT junction temperature estimation method proposed. The temperature of the IGBT can be adjusted by heating the plate flexibly. Since the on-state time of the IGBT pulse test is often hundreds of microseconds, the temperature rise caused by the power loss can be ignored. Therefore, for the double-pulse test platform, the heating plate temperature can be regarded as the IGBT junction temperature to be calibrated. Besides, the dc bus voltage V_{bus} and load current I_L can be set up to simulate IGBT characteristics under various operating conditions. The scheme of the double-pulse test is shown in Fig. 6.

The DUT is FF300R12ME4 of Infineon. The gate drive resistance is 10 Ω. The instruments and types of the double-pulse experiment platform are shown in Table I.

The prototype of the double-pulse experiment platform is shown in Fig. 7.

IGBT module is tested at various temperatures (25, 50, 75, 100, 125, and 150 °C), various load currents (30, 60, 90, 120, and 150A), various bus voltages (200, 300, 400, 500, 600 V), and different amounts of bond wires cut-off (bond wire free-fault, 1 bond wire lift-off, 2 bond wire lift-off, 3 bond wire lift-off, and 4 bond wire lift-off). Hence, a total of 750 IGBT on-state voltage and IGBT turn-ON gate voltage overshoot experimental data are collected and used as the model data set.

B. Experiment Results of the On-State Voltage Drop

The cover of IGBT module FF300R12ME4 is removed and the bond wires are shown in Fig. 8.

The IGBT junction temperatures are controlled by the heating plate. The bond wire failure is simulated by cutting off them. Fig. 8 shows that there are 6 bond wires in each IGBT chip. In total, 1, 2, 3, and 4 bond wires are cut off separately.

In this article, the on-state voltage drop of IGBT is monitored with the online measurement circuit proposed in [4]. The online monitoring circuit of IGBT on-state voltage drop is shown in Fig. 9.

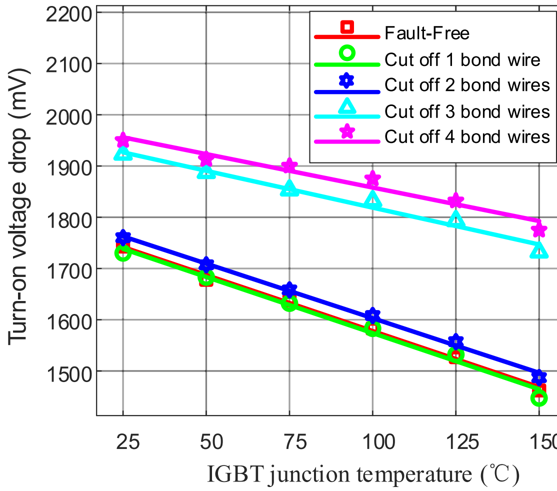

Fig. 10. On-state voltage drops with different amounts of bond wire faults and temperatures.

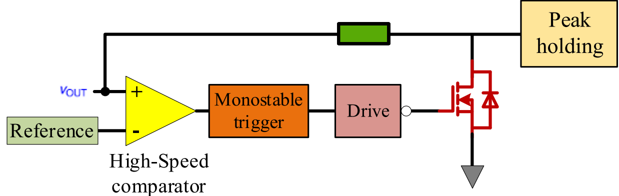

Fig. 11. Scheme of the pulse extraction.

TABLE II
PARAMETERS OF CRUCIAL PARTS AND THE TYPES OF INSTRUMENTS

Instruments	Types
NAND Gate	SN74LVC1G132
Isolated, single-channel driver	ADuM4121-1-EP
N-channel enhancement mode Field-Effect Transistor (FET)	PMV45EN
LDO Regulator	TPS7A6650H
High-speed comparator	TLV3501
Single re-triggerable monostable multivibrator with Schmitt trigger inputs	SN74LVC1G123
Rail-to-rail operational amplifier	OPA2350UA

With the online monitoring circuit shown in Fig. 9, the on-state voltage drops are measured with various temperatures and different amounts of bond wires cut-off. The experiment results of the on-state voltage drops are shown in Fig. 10.

As can be seen from Fig. 10, the on-state voltage drop of IGBT is significantly affected by temperature, which is consistent with the theoretical analysis. In addition, the on-state voltage drop of the IGBT at the same temperature is closely related to the state of the bond wires. However, the dependence of on-state voltage drop on the number of bond wire lift-off is not linear. The on-state voltage drop of IGBT with one or two bond wires did not differ much from those in healthy conditions, while the on-state voltage drops changed sharply when three or four bond wires lifts off. For example, at 100°, when three bond wires are broken, the on-state voltage deviation of IGBT reaches 200 mV. When two or fewer bond wires are broken, the on-state voltage deviation is less than 10 mV. It illustrates that there is an obvious nonlinear relationship between on-state voltage drop and the amount of bond wire lift-off. Therefore, it is difficult to monitor the temperature of IGBT based on a single analytical model.

C. Experiment Results of the Turn-On Gate Voltage Overshoot

Various amounts of bond wires are cut-off for experiments. The voltage between the gate and emitter of the IGBT is acquired by a voltage divider circuit. The output Vout of the voltage divider circuit is connected with the pulse extraction circuit, which extracts the narrow pulse including the turn-ON gate voltage overshoot $V_{\text{g_p}}$. The schematic of the pulse extraction circuit is shown in Fig. 11.

The output Vout of the differential voltage measuring circuit is connected with the in+ input of a high-speed comparator. High-speed comparator outputs high when the Vout is higher than the reference voltage, for instance, at zero level. The monostable trigger output a pulse whose duration is set according to the practical turn-ON transient. The monostable trigger turns OFF the auxiliary MOSFET by a drive circuit. Then, the output Vout of the differential voltage measuring circuit is transmitted to the peak holding circuit through a resistor. When the pulse of the monostable trigger is over, the input of the peak holding circuit is connected to GND.

The peak holding circuit of the gate signal is studied in detail [21], [22], [36]. The peak detector circuit consists of a differential amplifier, a peak detector, and a reset switch that is controlled by the gate voltage signal. The output of the peak detector is held on a memory capacitor for the entire on-state duration of the device. At the device turn-OFF transition, the memory capacitor is discharged via the reset switch controlled by the gate voltage.

A practical measurement circuit is built and the parameters of crucial parts and the types of instruments are shown in Table II.

With the pulse extraction circuit shown in Fig. 11, the turn-ON gate voltage overshoot of IGBT is measured at various temperatures and bond wire degradation. The dc bus voltage is set as 600 V and the load current is set as 150 A. The turn-ON gate voltage overshoots at various temperatures and bond wire degradation are shown in Fig. 12.

It can be seen from Fig. 12 that the turn-ON gate voltage overshoot of IGBT is strongly correlated with the temperature of IGBT. At the same time, the turn-ON gate voltage overshoot of IGBT is closely related to the bond wire failure, which is consistent with the theoretical analysis. Moreover, the turn-ON gate voltage overshoot of IGBT shows a nonlinear increasing trend with the increase of the amount of bond wire lift-off. Therefore, it is difficult to decouple the effect of bond wire failure in temperature monitoring of IGBT based on turn-ON gate voltage overshooting alone.

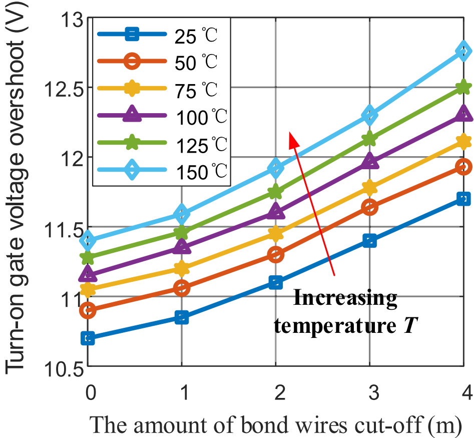

Fig. 12. Turn-ON gate voltage overshoots at various temperatures and bond wire degradation.

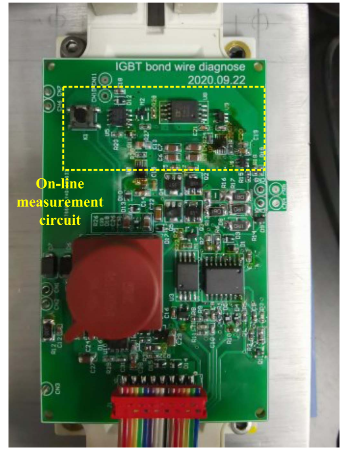

Fig. 13. On-line measurement circuit for the turn-ON gate voltage overshoot and on-state voltage drop.

D. Practical Implementation and Verification With Neural Network Model Proposed

To measure the on-state voltage drop and turn-ON gate voltage overshooting, the practical implementation for Figs. 9 and 11 is built and shown in Fig. 13.

With the online measurement circuit, the temperature-sensitive parameters, turn-ON gate voltage overshoot, and on-state voltage drop are measured at various collector-emitter voltages, load currents IGBT junction temperatures, and amounts of bond wire lift-off. The temperatures are set as 25°, 50°, 75°, 100°, 125°, and 150°, respectively. The collector currents are set as 30 A, 60 A, 90 A, 120 A, and 150 A, respectively. The collector-emitter voltages are set as 200 V, 300 V, 400 V, 500 V, and 600 V, respectively. The bond wire conditions are healthy, 1, 2, 3, and 4 bond wires cut-off, respectively. Hence, 750 sets of data need to be tested in advance and are divided into three categories, namely training set, test set, and validation set. These three datasets account for 70%, 15%, and 15% of the total data, respectively.

The neural network model is shown in Fig. 14.

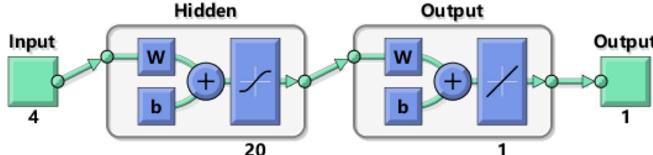

Fig. 14. Neural network model for IGBT junction temperature estimation.

TABLE III
WHOLE PERFORMANCE, TRAIN PERFORMANCE, VALIDATION PERFORMANCE, AND TEST PERFORMANCE WITH VARIOUS NUMBERS OF HIDDEN LAYERS

Hidden Layer Size	Whole performance	Train Performance	Validation Performance	Test Performance
2	97.4316	92.2298	102.9103	116.0742
5	39.2004	35.8041	47.8784	46.2714
10	22.5918	20.4490	29.6274	25.4928
15	21.1601	20.0678	23.7514	23.6340
20	**11.6876**	**10.8606**	**13.2691**	**13.9411**
22	12.5251	10.3242	15.5353	19.7207
25	16.9691	17.1078	16.4236	16.8710
30	15.2891	13.4066	20.7485	18.5587
40	14.9519	11.9448	25.3280	18.5200

In Fig. 14, 4 input parameters are collector-emitter voltages, load currents, turn-ON gate voltage overshoot, and on-state voltage drop, and 1 output parameter is IGBT junction temperature. It is important to note here that the bond wire condition is not yet used as an input parameter in the input layer. In this way, the bond wire degradation can be decoupled.

To test the optimal number of hidden layers in the neural network, various numbers of hidden layers of 2–40 are tested. The performance is the mean squared error of data set mapping. The whole performance, train performance, validation performance, and test performance are listed in Table III.

As can be seen from Table III, the number of hidden layers in the middle of the neural network used for IGBT junction temperature estimation directly affects the performance of the neural network model. When the number of layers is 2, the fitting error is the largest. When the number of layers is 20, the performance of whole sets, validation sets, and test sets reaches 11.6876, 13.2691, and 13.9411, which is the smallest among the various hidden layers. When the number of hidden layers is greater than 20, the performance of the training set will fluctuate slightly, but the performances of whole sets, validation sets, and test sets are larger than that of the number of layers is 20. Therefore, the number of hidden layers 20 can be considered the best number of hidden layers for IGBT junction temperature monitoring.

For the BP neural network proposed in this article, the output error of the neural network model is obtained. When the output error does not change for 6 consecutive iterations, the training is terminated and the required neural network model is determined. The gradient and error invariant epochs in the iteration process are shown in Fig. 15.

Fig. 15 shows that after 78 epochs, the neural network model of junction temperature estimation with a set threshold can be obtained. The fitting results of the neural network with training

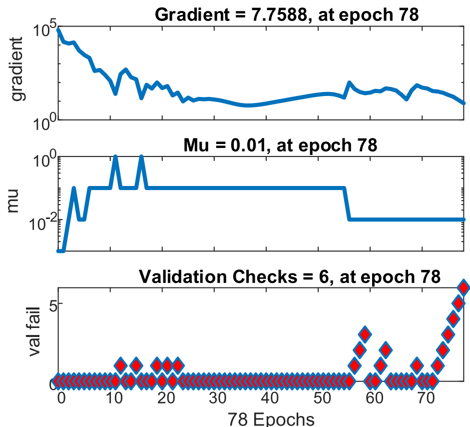

Fig. 15. Gradient and error invariant epochs in the iteration process.

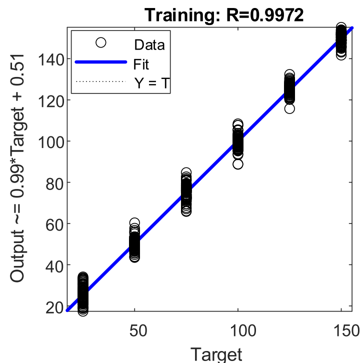

Fig. 16. Fitting results of the neural network with training sets.

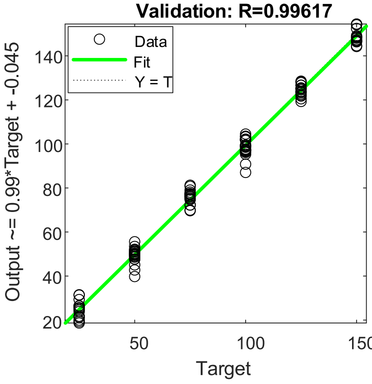

Fig. 17. Fitting results of the neural network with validation sets.

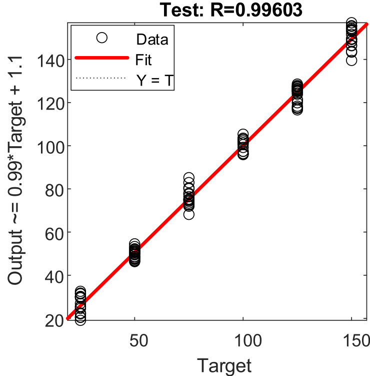

Fig. 18. Fitting results of neural network with test sets.

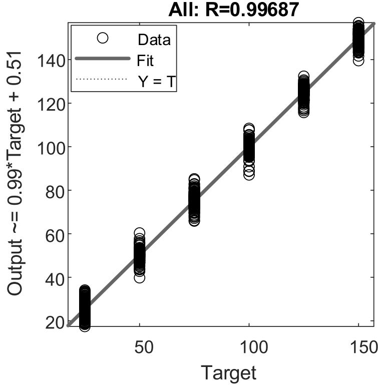

Fig. 19. Fitting results of the neural network with whole sets.

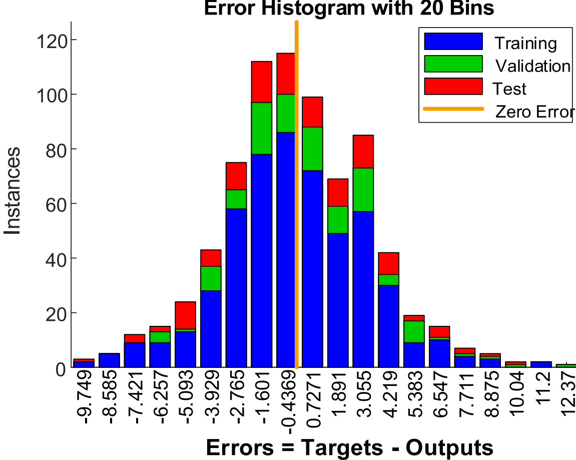

Fig. 20. Error histogram of the training set, validation set, and test set of the neural network.

sets, validation sets, test sets, and whole sets are shown in Figs. 16 –19.

Figs. 16–19 illustrate that the coefficient R of determination of training sets, validation sets, test sets, and whole sets are more than 0.996. This indicates that the proposed IGBT junction temperature estimation method based on the neural network has high accuracy. More critically, the bond wire conditions are not involved in the training of the neural network.

The error histogram of the training set, validation set, and test set of the neural network is shown in Fig. 20.

As can be seen from the error distribution diagram in Fig. 20, the fitting error of more than 90% of the data in the fitting result of this model is less than 4.219°, indicating high accuracy. The mean squared error during each epoch is shown in Fig. 21.

Fig. 21 illustrates that the mean squared error decreases gradually, with the increase of iteration epochs. The best validation performance is 12.4026 at epoch 72.

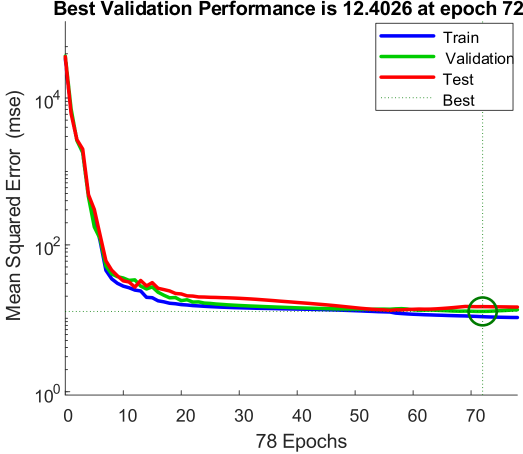

Fig. 21. Mean squared error during each epoch.

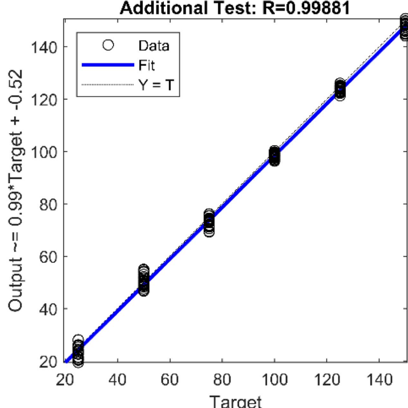

Fig. 22. Additional test results of the trained BP neural network model with healthy bond wire.

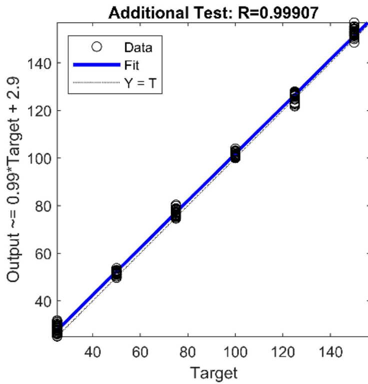

Fig. 23. Additional test results of the trained BP neural network model with 1 bond wire failure.

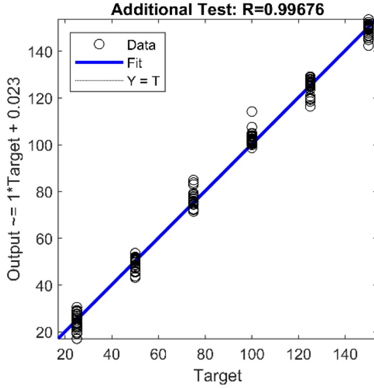

Fig. 24. Additional test results of the trained BP neural network model with 2 bond wire failure.

For practical implementation, the turn-ON gate voltage overshoot and on-state voltage drop can be acquired with the online monitoring circuit of the IGBT on-state voltage drop shown in Fig. 9 and the scheme of the pulse extraction shown in Fig. 11. Before the method is applied in a live converter, the experimental data of various voltages, various currents, various temperatures, and various bond wire degradation are obtained by a double pulse test. A large number of double-pulse experimental data are used to train and form BP neural networks. In practical monitoring applications, the turn-ON gate voltage overshoot, on-state voltage drop, bus voltage, and load current are measured online and put into the BP neural network structure for IGBT temperature monitoring in Fig. 5. The junction temperature of IGBT can be obtained by BP neural network trained.

E. Verification With Various Bond Wire Degradation

Through the above-mentioned training, BP neural network is formed. In order to verify the independence of the BP neural network on the bond wire failure, the data under various degradation of the bond wire are put into the trained BP neural network model for test and verification. The additional test results are shown in Figs. 22 –26.

Figs. 22–26 show that the BP neural network proposed in this study can effectively monitor IGBT temperature regardless of whether the IGBT bond wire is healthy or partially failed. The coefficient R of determination of additional test results is more than 0.994. Therefore, the method proposed can monitor the IGBT junction temperatures without the influence of bond wire degradation.

F. Comparison of the Existing TSEPs Using ANN

The BP neural network proposed utilizes the on-state voltage drop and the turn-ON gate voltage overshoot for the IGBT junction temperature estimation. In order to verify the rationality of the proposed method, ANN was used to analyze the on-state voltage drop and the turn-ON gate voltage for comparison.

First, the on-state voltage drops combined neural network is analyzed. The BP neural network structure combined on-state voltage drops for IGBT temperature monitoring is shown in Fig. 27.

By using the neural network structure shown in Fig. 27 and taking the on-state voltage and load current of IGBT as model inputs, the neural network for estimating the junction temperature of IGBT is constructed. The estimation accuracy of the neural network for estimating the junction temperature of

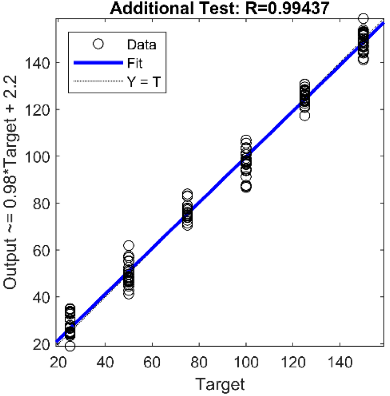

Fig. 25. Additional test results of the trained BP neural network model with 3 bond wire failure.

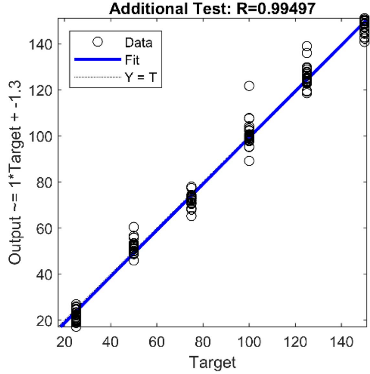

Fig. 26. Additional test results of the trained BP neural network model with 4 bond wire failure.

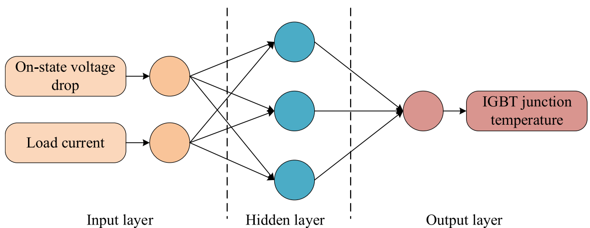

Fig. 27. BP neural network structure combined on-state voltage drops for IGBT temperature monitoring.

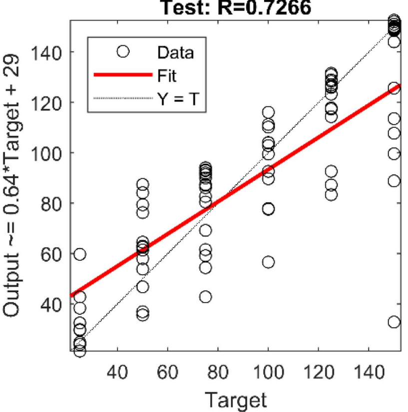

Fig. 28. Fitting results of the neural network with only on-state voltage drops used.

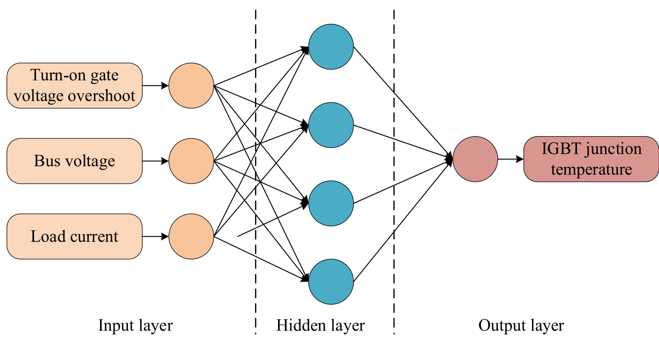

Fig. 29. BP neural network structure combined the turn-ON gate voltage overshoot for IGBT temperature monitoring.

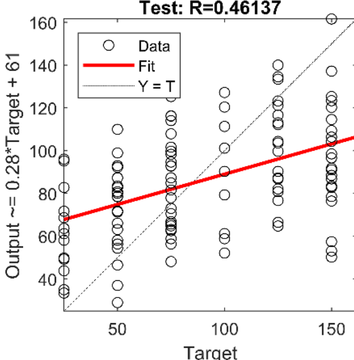

Fig. 30. Fitting results of the neural network with only the turn-ON gate voltage overshoot used.

IGBT is analyzed. The fitting result of the test sets is shown in Fig. 28.

Fig. 28 shows that the coefficient R of determination of test results is 0.7266. Besides, the dispersion distance between experimental data points and the fitting line is relatively large. The maximum temperature estimation error is more than 35°. Therefore, it is not feasible to estimate junction temperature by only using on-state voltage drops and neural networks.

On the other hand, the turn-ON gate voltage overshoot combined neural network is analyzed. The BP neural network structure combined with the turn-ON gate voltage overshoot for IGBT temperature monitoring is shown in Fig. 29.

By using the neural network structure shown in Fig. 29 and taking the turn-ON gate voltage overshoot, bus voltage, and load current of IGBT as model inputs, the neural network for estimating the junction temperature of IGBT is constructed. The estimation accuracy of the neural network for estimating the junction temperature of IGBT is analyzed. The fitting result of the test sets is shown in Fig. 30.

Fig. 30 shows that the coefficient R of determination of test results is 0.4614. Besides, the dispersion distance between

experimental data points and the fitting line is relatively large. The maximum temperature estimation error is more than 61°. Therefore, it is not feasible to estimate junction temperature with neural networks only using turn-ON gate voltage overshoot.

It can be seen from the above-mentioned experimental results that both the on-gate voltage overshoot and on-state voltage of IGBT belong to thermo-sensitive electric parameters, that is, they are closely related to temperature. At the same time, they are also affected by bond wire failure, and the relationship with bond wire failure is nonlinear. If any single parameter is selected for temperature monitoring, the influence of the bond wire cannot be avoided. Moreover, it is difficult to establish an accurate mathematical analytical model for temperature monitoring because of the nonlinear relationships. The method of IGBT temperature monitoring based on the neural network proposed in this article can effectively establish the nonlinear mapping relationship between temperature and electrical parameters, and realize accurate junction temperature monitoring without the influence of IGBT bond wire degradation.

IV. Conclusion

In this article, a novel junction temperature estimation method independent of bond wire degradation for IGBT has been proposed with analysis and experimental validation presented. The on-state voltage drop is strongly dependent on the IGBT junction and bond wire degradation. Besides, the turn-ON gate voltage overshoot is also influenced by the IGBT junction and bond wire degradation. As a result, the on-state voltage drop and turn-ON gate voltage overshoot are combined by a BP neural network algorithm, which can eliminate the influence of bond wire degradation and accurately monitor the junction temperature of the IGBT. A practical measurement implementation has also been discussed in this article. The method proposed is verified by the experiments. The fitting error of more than 90% of the data in the fitting result of this model is less than 4.219°, and the validation performance is 12.4026 at epoch 72. It has been shown that the method proposed has the advantages of being noninvasive, having high precision and independence on the bond wire degradation. It is promising and suitable for long-term IGBT junction temperature monitoring.

References

[1] P. Asimakopoulos, K. Papastergiou, T. Thiringer, M. Bongiorno, and G. Le Godec, "On V_{ce} method: In situ temperature estimation and aging detection of high-current IGBT modules used in magnet power supplies for particle accelerators," *IEEE Trans. Ind. Electron.*, vol. 66, no. 1, pp. 551–560, Jan. 2019.

[2] S. Yang, A. Bryant, P. Mawby, D. Xiang, L. Ran, and P. Tavner, "An industry-based survey of reliability in power electronic converters," *IEEE Trans. Ind. Appl.*, vol. 47, no. 3, pp. 1441–1451, May/Jun. 2011.

[3] Society of Automotive Engineers (US-SAE), *Handbook for Robustness Validation of Automotive Electrical/Electronic Modules*. Frankfurt, Germany: ZVEL, Jun. 2008.

[4] Y. Yang, Q. Zhang, and P. Zhang, "A fast IGBT junction temperature estimation approach based on on-state voltage drop," *IEEE Trans. Ind. Appl.*, vol. 57, no. 1, pp. 685–693, Jan./Feb. 2021.

[5] Y. Yang, Q. Zhang, and P. Zhang, "A novel on-line IGBT junction temperature measurement method based on on-state voltage drop," in *Proc. 22nd Int. Conf. Elect. Mach. Syst.*, 2019, pp. 1–6.

[6] Y. Yang and P. Zhang, "A novel in situ IGBT and FWD junction temperature estimation technique for IGBT module based on on-state voltage drop measurement," in *Proc. IEEE Energy Convers. Congr. Expo.*, 2020, pp. 2529–2534.

[7] X. Perpiñà, J. F. Serviere, J. Saiz, D. Barlini, M. Mermet-Guyennet, and J. Millán, "Temperature measurement on series resistance and devices in power packs based on on-state voltage drop monitoring at high current," *Microelectronics Rel.*, vol. 46, no. 9, pp. 1834–1839, Sep. 2016.

[8] L. Dupont, Y. Avenas, and P. O. Jeannin, "Comparison of junction temperature evaluations in a power IGBT module using an IR camera and three thermo-sensitive electrical parameters," *IEEE Trans. Ind. Appl.*, vol. 49, no. 4, pp. 1599–1608, Jul./Aug. 2013.

[9] N. Baker and F. Iannuzzo, "The temperature dependence of the flatband voltage in high-power IGBTs," *IEEE Trans. Ind. Electron.*, vol. 66, no. 7, pp. 5581–5584, Jul. 2019.

[10] R. Mandeya, C. Chen, V. Pickert, and R. T. Naayagi, "Prethreshold voltage as a low-component count temperature sensitive electrical parameter without self-heating," *IEEE Trans. Power Electron.*, vol. 33, no. 4, pp. 2787–2791, Apr. 2018.

[11] J. A. Butron Ccoa, B. Strauss, G. Mitic, and A. Lindemann, "Investigation of temperature sensitive electrical parameters for power semiconductors (IGBT) in real-time applications," in *Proc. Int. Exhib. Conf. Power Electron., Intell. Motion, Renewable Energy, Energy Manage.*, 2014, pp. 1–9.

[12] C. H. van der Broeck, A. Gospodinov, and R. W. de Doncker, "IGBT junction temperature estimation via gate voltage plateau sensing," *IEEE Trans. Ind. Appl.*, vol. 54, no. 5, pp. 4752–4763, Sep./Oct. 2018.

[13] V. K. Sundaramoorthy, E. Bianda, M. Kamel, G. J. Riedel, and I. Nistor, "Online junction temperature estimation for IGBT modules with paralleled semiconductor chips," in *Proc. 7th IET Int. Conf. Power Electron., Mach. Drives*, 2014, pp. 1–5.

[14] A. Bryant et al., "Investigation into IGBT dV/dt during turn-off and its temperature dependence," *IEEE Trans. Power Electron.*, vol. 26, no. 10, pp. 3019–3031, Oct. 2011.

[15] Y. Chen et al., "A thermo-sensitive electrical parameter with maximum dIC/dt during turn-off for high power trench/field-stop IGBT modules," in *Proc. IEEE Appl. Power Electron. Conf. Expo.*, 2016, pp. 499–504.

[16] B. Ji, V. Pickert, W. Cao, and B. Zahawi, "In situ diagnostics and prognostics of wire bonding faults in IGBT modules for electric vehicle drives," *IEEE Trans. Power Electron.*, vol. 28, no. 12, pp. 5568–5577, Dec. 2013.

[17] Z. Xu, F. Xu, and F. Wang, "Junction temperature measurement of IGBTs using short-circuit current as a temperature-sensitive electrical parameter for converter prototype evaluation," *IEEE Trans. Ind. Electron.*, vol. 62, no. 6, pp. 3419–3429, Jun. 2015.

[18] B. Wang, Y. Tang, and M. Chen, "Study on electric characteristic of IGBT at different junction temperature," in *Proc. Asia-Pacific Power Energy Eng. Conf.*, 2011, pp. 1–4.

[19] B. Jayant Baliga, "Temperature behavior of insulated gate transistor characteristics," *Solid-State Electron.*, vol. 28, pp. 289–297, 1985.

[20] N. Baker, S. Munk-Nielsen, F. Iannuzzo, and M. Liserre, "Online junction temperature measurement using peak gate current," in *Proc. IEEE Appl. Power Electron. Conf. Expo.*, 2015, pp. 1270–1275.

[21] N. Baker, L. Dupont, S. Munk-Nielsen, F. Iannuzzo, and M. Liserre, "IR camera validation of IGBT junction temperature measurement via peak gate current," *IEEE Trans. Power Electron.*, vol. 32, no. 4, pp. 3099–3111, Apr. 2017.

[22] N. Baker, S. Munk-Nielsen, F. Iannuzzo, and M. Liserre, "IGBT junction temperature measurement via peak gate current," *IEEE Trans. Power Electron.*, vol. 31, no. 5, pp. 3784–3793, May 2016.

[23] H. Kuhn and A. Mertens, "On-line junction temperature measurement of IGBTs based on temperature sensitive electrical parameters," in *Proc. 13th Eur. Conf. Power Electron. Appl.*, 2009, pp. 1–10.

[24] W. Shi et al., "A current sensorless IGBT junction temperature extraction method via parasitic parameters between power collector and auxiliary collector," in *Proc. IEEE Appl. Power Electron. Conf. Expo.*, Mar. 2017, pp. 3021–3026.

[25] D. Barlinia, M. Ciappaa, A. Castellazzia, M. Mermet-Guyennetb, and W. Fichtnera, "New technique for the measurement of the static and of the transient junction temperature in IGBT devices under operating conditions," *Microelectronics Rel.*, vol. 46, no. 9, pp. 1772–1777, Sep. 2006.

[26] J. Liu, G. Zhang, Q. Chen, L. Qi, Y. Geng, and J. Wang, "In situ condition monitoring of IGBTs based on the miller plateau duration," *IEEE Trans. Power Electron.*, vol. 34, no. 1, pp. 769–782, Jan. 2019.

[27] H. Luo, Y. Chen, P. Sun, W. Li, and X. He, “Junction temperature extraction approach with turn-off delay time for high-voltage high-power IGBT modules,” *IEEE Trans. Power Electron.*, vol. 31, no. 7, pp. 5122–5132, Jul. 2016.

[28] D. Herwig, T. Brockhage, and A. Mertens, “Combining multiple temperature-sensitive electrical parameters using artificial neural networks,” in *Proc. 22nd Eur. Conf. Power Electron. Appl.*, 2020, pp. 1–10.

[29] J. Miao, Q. Yin, H. Wang, Y. Liu, H. Li, and S. Duan, “IGBT junction temperature estimation based on machine learning method,” in *Proc. IEEE 9th Int. Power Electron. Motion Control Conf.*, 2020, pp. 1–5.

[30] C. Dong and P. Mao, “The junction temperature measurement of insulated gate bipolar transistor based on multi-layer feed-forward neural network is presented,” in *Proc. IEEE Int. Conf. Mechatronics Automat.*, 2020, pp. 136–140.

[31] Y. Yuan, L. Yunfei, and W. Yang, “Online junction temperature estimation system for IGBT based on BP neural network,” in *Proc. IEEE 5th Int. Conf. Electron. Technol.*, 2022, pp. 526–531.

[32] X. Bie, F. Qin, T. An, J. Zhao, and C. Fang, “Numerical simulation of the wire bonding reliability of IGBT module under power cycling,” in *Proc. 18th Int. Conf. Electron. Packag. Technol.*, 2017, pp. 1396–1401.

[33] Y. Yang and P. Zhang, “In situ junction temperature monitoring and bond wire detecting method based on IGBT and FWD on-state voltage drops,” *IEEE Trans. Ind. Appl.*, vol. 58, no. 1, pp. 576–587, Jan./Feb. 2022.

[34] Y. Yang and P. Zhang, “A novel bond wire fault detection method for IGBT modules based on turn-on gate voltage overshoot,” *IEEE Trans. Power Electron.*, vol. 36, no. 7, pp. 7501–7512, Jul. 2021.

[35] T. Gu, “Study and optimization of IGBT half-bridge module parasitic inductance,” Zhejiang University, Hangzhou, China, 2014.

[36] V. K. Sundaramoorthy, E. Bianda, R. Bloch, and F. Zurfluh, “Simultaneous online estimation of junction temperature and current of IGBTs using emitter-auxiliary emitter parasitic inductance,” in *Proc. Int. Exhib. Conf. Power Electron., Intell. Motion, Renewable Energy, Energy Manage.*, 2014, pp. 1–8.

Yanyong Yang (Member, IEEE) received the B.Eng. and master’s degrees from Zhejiang University, Hangzhou, China, in 2015 and 2018, respectively, and the Ph.D. degree from Tsinghua University, Beijing, China, in 2022, all in electrical engineering.

He is currently a Postdoctoral Research Fellow with the Department of Electrical Engineering, Beihang University, Beijing, China. His current research interests include condition monitoring, thermal management, diagnostics, and prognostics techniques for power electronic devices in real-time applications.

Dr. Yang was the recipient of the best paper awards from the IEEE IAS Society.

Xiaofeng Ding (Member, IEEE) received the B.S., M.S., and Ph.D. degrees in electrical engineering from Northwestern Polytechnical University, Xi’an, China, in 2005, 2008, and 2011, respectively.

From 2008 to 2010, he was a joint education Ph.D. with the University of Michigan-Dearborn, Dearborn, MI, USA. He is currently a Professor and the Head of the Department of Electrical Engineering, Beihang University, Beijing, China. His research interests include permanent magnet electric machines and their drives based on wide bandgap power devices, such as silicon carbide, and gallium nitride devices.

Pinjia Zhang (Senior Member, IEEE) received the B.Eng. degree from Tsinghua University, Beijing, China, in 2006, and the master’s and Ph.D. degrees from the Georgia Institute of Technology, Atlanta, GA, USA, in 2009 and 2010, respectively, all in electrical engineering.

From 2010 to 2015, he was with the Electrical Machines Laboratory, GE Global Research Center, Niskayuna, NY, USA. Since 2015, he has been with the Department of Electrical Engineering, Tsinghua University, as an Associate Professor. His research interests include condition monitoring, diagnostics, and prognostics techniques for electrical assets.